Contribution from the Department of Chemistry,
University of Alberta, Edmonton, Alberta, Canada T6G 2G2

Phosphoranes. 10. Barriers to Five-Coordinate Permutations and/or Rotation of the Thiomethyl Group in Fluoro- and (Trifluoromethyl)phosphoranes by Means of Dynamic NMR Studies[1]

RONALD G. CAVELL,* KWAT I. THE, J. ANDREW GIBSON, and NONITA T. YAP

Received March 27, 1979

Line-shape analyses of the proton-decoupled ^{31}P NMR spectra of $F_4P(SCH_3)$, $CF_3PF_3(SCH_3)$ (including in this case ^{19}F dynamic behavior of the CF_3 region), $(CF_3)_2PF_2(SCH_3)$, and $(CF_3)_3PF(SCH_3)$ have been carried out. Two processes can be distinguished in $CF_3PF_3(SCH_3)$: the five-coordinate permutation (i.e., Berry pseudorotation (BPR)) and the rotation of the SCH_3 group about the P–S bond. Respective barriers ($\Delta G_{298}^{\ddagger}$) are 12.8 (±0.6) and 10.2 (±0.3) kcal. The $\Delta G_{298}^{\ddagger}$ values of 10.0 (±0.2) and 11.0 (±0.3) kcal/mol obtained for the observable process in $(CF_3)_2PF_2(SCH_3)$ and $CH_3(CF_3)PF_2(SCH_3)$, respectively, are attributed to a pure rotation process since there is no spectral evidence to support CF_3–F positional interchange. The processes which equilibrate the three distinguishable fluorine environments in $F_4P(SCH_3)$ (a pair of equatorial fluorine atoms and two distinct axial environments) yield only one barrier of 11.0 (±0.3) kcal, *larger* than that reported for $F_4PN(CH_3)_2$. Detailed analysis of the line shapes and the above behavior of $CF_3PF_3(SCH_3)$, wherein the processes are separable, strongly suggest that the permutational process in $F_4P(SCH_3)$ is *not* concerted (i.e., BPR is not intimately coupled with rotation about the P–S bond) but rather involves uncorrelated independent rotation and pseudorotation processes represented by an overall barrier. The barrier to exchange (permutation of CF_3 groups) in $(CF_3)_3PF(SCH_3)$ is 11.5 kcal.

Introduction

As part of a study[2] of permutational processes in five-coordinate phosphoranes with monofunctional substituents, we have undertaken a study of the energetics of the NMR-observable processes (axial–equatorial permutation and/or P–S bond rotation) in the (methylthio)phosphoranes $F_4P(SCH_3)$,[3] $CF_3PF_3(SCH_3)$, $CF_3(CH_3)PF_2(SCH_3)$, $(CF_3)_2PF_2(SCH_3)$, and $(CF_3)_3FP(SCH_3)$.[4] The angular SCH_3 group introduces magnetic nonequivalence in the biaxial F environments in all but the last compound. This nonequivalence permits the determination, in favorable cases, of a barrier for the P–S bond rotation process, a process which has not hitherto been extensively analyzed.

Results and Discussion

A. Tetrafluoro(methylthio)phosphorane. The limiting low-temperature ^{19}F NMR spectrum of $F_4P(SCH_3)$ at 183 K agrees with that described previously,[5] showing three distinct fluorine environments. The coupling constants obtained herein from ^{19}F and ^{31}P NMR spectroscopy, confirmed by calculation of the spectrum with NUMARIT,[6] are given in Table I and are in fair agreement with those reported earlier.[7] The discrepancies may be due to the absence of a signal lock in the previous work. The proton-decoupled ^{31}P low-temperature limiting NMR spectrum of $F_4P(SCH_3)$ (Figure 1) consists of 12 lines: a triplet of doublets of doublets which is consistent with the assignments based on the ^{19}F NMR spectrum.

The static ground-state structure of $F_4P(SCH_3)$ is most likely a trigonal bipyramid[3] with the SCH_3 group located in an equatorial position and lying out of the equatorial plane in such a way as to create magnetically nonequivalent axial fluorine environments.[3,5]

Because the axial fluorine environments are not equivalent, the exchange process has two observable features: permutation of axial and equatorial fluorine environments and mutual exchange of the unique axial fluorine environments. The latter process is equivalent to rotation of the SCH_3 group about the P–S bond (or to inversion at sulfur[8]). Regardless of the underlying mechanism, it is clear that in order for the observed spectrum to be reproduced both "pseudorotation" (i.e., Berry pseudorotation[10] (BPR) or its permutational equivalent[11]) and P–S bond rotation must cease. The process may be viewed in two ways. In the first a correlated motion is visualized in which the fluorine permutations are coupled to P–S rotation such that axial–equatorial fluorine interchange is accompanied by 90° rotation about the P–S bond, thus destroying the equivalence of the equatorial fluorine atoms upon their transformation into the axial environment. A kinetic magnetization-transfer matrix[12] based on this model is given in Table II. The magnetization-transfer possibilities represented by elements in this matrix are multiplied by a rate constant which is the unique rate for the concerted process. Alternatively we may consider both processes to be independent (noncorrelated) and to proceed with an overall rate which is the combined rate for pseudorotation and rotation. A matrix constructed on this concept in which the relative rates of rotation and pseudorotation are 1:4 is given in Table III. Both cases involve magnetization transfer between the same lines, but the different internal relative rates make the elements in the kinetic transfer matrix different. The gross features of the spectrum are accounted for by each of these matrices (Figure 2). Matrices derived for non-Berry processes do not fit the spectrum; hence such processes may be excluded. We cannot of course distinguish between equivalent processes or nonobservable processes.[10,11,13-15]

Detailed examination of the behavior of the spectra in an intermediate exchange region suggests that the correlated and noncorrelated processes may be distinguishable as illustrated in Figure 3. The former model yields calculated spectra which show a prominence of the central line which is not present in the experimental spectrum, and we suggest that the line shape is better reproduced by the matrix for the noncorrelated processes. It is possible that the subtle difference in the line shapes of $F_4P(SCH_3)$ models is due to the use of approximate symmetrized wave functions instead of the true eigenfunctions (wherein the mixing of states is accounted for). This possibility, and the fact that only one barrier value for ostensibly two processes is obtained, renders the conclusion less convincing than the case of $CF_3PF_3(SCH_3)$, discussed below, where the barriers are separable.

Thermodynamic parameters extracted from Arrhenius and Eyring equations[4] are given in Table IV. In all cases barrier comparisons are based on the more reliable $\Delta G^{\ddagger}$ (evaluated at 298 K) values rather than E_a.[17] Notably the barrier to pseudorotation in $F_4P(SCH_3)$ is larger than that obtained[18] for $F_4PN(CH_3)_2$ in contrast to the qualitative estimate of a smaller relative barrier to exchange in $F_4P(SCH_3)$ estimated earlier.[18] This emphasizes the value of proper barrier analysis.

0020-1669/79/1318-3400$01.00/0

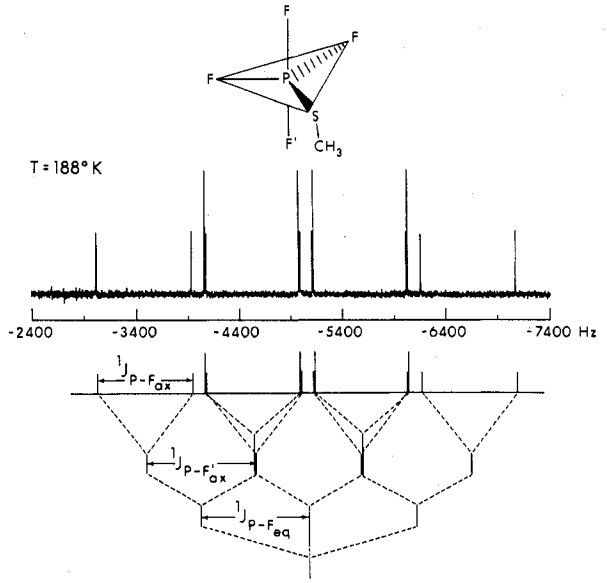

Figure 1. $^{31}P\{^1H\}$ (36.4 MHz) FT NMR spectrum of $F_4P(SCH_3)$ at 188 K. The stick diagram shows the spin-splitting patterns. The scale gives offset frequencies corrected to P_4O_6 reference measured with heteronuclear lock system.

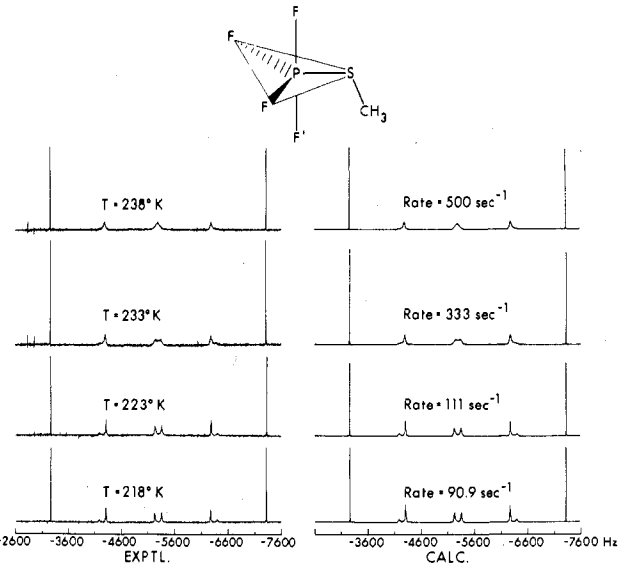

Figure 2. Temperature-dependent $^{31}P\{^1H\}$ FT NMR spectra of $F_4P(SCH_3)$ in the intermediate exchange region. The calculated spectra were obtained with the uncorrelated matrix. The frequency scale gives the offset frequencies relative to the P_4O_6 reference.

B. $(CF_3)_2PF_2(SCH_3)$ and $CF_3(CH_3)PF_2(SCH_3)$. These two compounds are characterized by magnetically nonequivalent (axial) fluorine atoms in the limiting low-temperature spectrum. The only differentiable NMR permutation process is mutual axial F exchange, equivalent to P–S bond rotation,[8] and, in order for the spectrum to be reproduced, the permutation matrix for each system, given in Table V, is repeated seven or four times, respectively, for groups of lines spaced by $^2J_{PF}$. The CF_3 group is assumed to be freely rotating. The limiting low-temperature spectra (parameters in Table I) are in agreement with a trigonal-bipyramidal ground-state structure with SCH_3 occupying an equatorial site (along with the two CF_3 groups) and lying out of the equatorial plane. While the NMR data do not exclude the possibility that the nonequivalent fluorine atom environments in $CH_3(CF_3)PF_2(SCH_3)$ arise from a square-pyramidal structure such as C (Figure 4), the required CF_3 inequivalence is not observed in the case of $(CF_3)_2PF_2(SCH_3)$ and structures A and B seem to be the most reasonable choices. It is notable that $^2J_{PF}$ and ϕ_{CF_3} are temperature invariant, suggesting that the environment of the CF_3 group is unchanged throughout the experimental temperature range. The normal-temperature values of ϕ_F and $^1J_{PF}$ are weighted averages of the low-temperature limiting values, indicating that exchange averaging is responsible for the behavior of the spectrum.

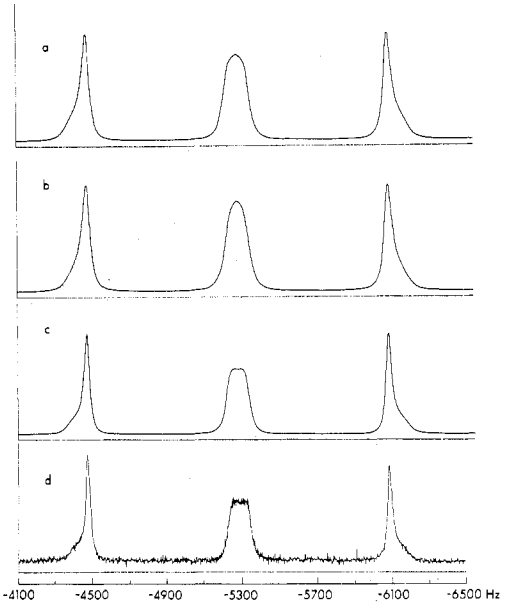

Figure 3. Details of the central region (−4100 to −6500 Hz) of the ^{31}P NMR spectrum calculated for different exchange matrices for $F_4P(SCH_3)$. Parts a–c describe (a) coupled BPR and P–S bond rotation, (b) uncorrelated BPR (90%) and P–S bond rotation (10%), and (c) a combination of uncorrelated BPR (80%) and P–S bond rotation (20%), and part d is the experimental spectrum at 238 K.

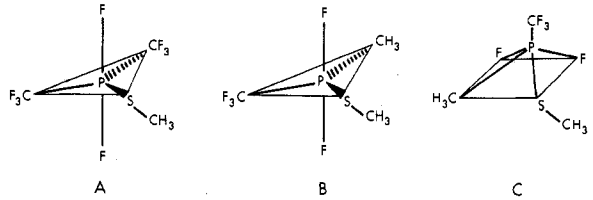

Figure 4. Structure of $(CF_3)_2PF_2(SCH_3)$ (A) and possible structures of $CF_3(CH_3)PF_2(SCH_3)$ (B and C).

The exchange process responsible for the averaging process in these two compounds may be cessation of (a) the free rotation of the SCH_3 group about the P–S bond[8] or (b) an intramolecular exchange process which interchanges the fluorine environments relative to a fixed SCH_3 group (with the CH_3 out of the equatorial plane). The latter intermolecular exchange process cannot be a BPR (or the permutationally equivalent turnstile rotation (TR)) type because these processes cannot interchange the two axial directly bound fluorine atoms while maintaining the SCH_3 group in a fixed orientation. A third alternative (c) is a concerted mechanism in which the P–S bond rotation is closely coupled with the ligand positional exchange process. Kinetic magnetization-transfer matrices are identical for processes a and c, and these processes cannot be differentiated. In view of the indication above that BPR and P–S bond rotation are not concerted in $F_4P(SCH_3)$, we favor the simplest process (a), and the derived thermodynamic parameters (Table IV) are attributed to the P–S bond rotation barrier.

C. (Trifluoromethyl)trifluoro(methylthio)phosphorane. The ^{19}F NMR spectrum of $CF_3PF_3(SCH_3)$ (Figure 5) at 273 K (the highest temperature investigated) showed three features: (a) a doublet of quartets due to the CF_3 group, (b) a very

Table I. NMR Data for (Methylthio)fluorophosphoranes

compd	T, °C	chem shift				coupling const[d]								
		τ[a]	ϕ_F[b]	ϕ_{CF_3}[b]	$\sigma^{31}P$[c]	$^1J_{P-F_{eq}}$	$^1J_{P-F_{ax}}$	$^2J_{P-F}$	$^2J_{P-H}$	$^3J_{P-H}$	$^3J_{F-H}$	$^4J_{F-H}$	$^2J_{F-F}$	$^3J_{F-F}$
$F_4P(SCH_3)$[e]	0	8.07	45.5	...	146.2	1032[f]	...	...	...	21.8	...		...	...
	−90		14.1[g]				1055[j]						90.5[l]	
			7.5[h]				917[k]						105.0[m]	
			58.2[i]			1044							19.0[n]	
$CF_3PF_3(SCH_3)$	0	7.65		69.2	140.0		1028.8[f]	168.0	...	23.2	...	1.8	82.0[l]	12.0[f]
	−90		16.1[g]				927[j]	168.8					71.0[m]	16.0[o]
			24.8[h]			...	1057[k]						41.0[n]	4.0[p]
			76.2[i]			1081.5[i]	...							16.0[q]
$(CF_3)_2PF_2(SCH_3)$	+33	7.72	41.0	67.4	142.4		924[f]	130.5	...	22.2	...	1.7	...	16.5
	−100		38.7			...	867[j]							
			45.1			...	986[k]							
$(CH_3)(CF_3)PF_2(SCH_3)$	+30	8.06[r] 7.18[s]	20.4	69.8	127.2	...	804	148	18.0	20.0	12.2	1.7	...	15.0
	−90		18.0[g]				728[j]						50[n]	
			26.4[h]				860[k]							
$(CF_3)_3PF(SCH_3)$	+30	7.92	1.0	61.7	161.5		980	103.7	...	19.2	...	2.5		16.5
	−6			60.3[t]	161.5		975	107.5[f]						
	−70			59.9[v]				33.8[t] 134[u]						13

[a] Ppm relative to internal tetramethylsilane, $\tau = 10.0$. [b] Ppm relative to internal CCl_3F with positive values indicating resonance to high field of the standard. [c] Ppm relative to P_4O_6 as external (capillary) reference,[26] positive values indicating resonance to high field of the standard. [d] In units of hertz. [e] Parameters are in fair agreement with those given in ref 5. [f] Average value. [g] Unique axial environment of one F (type A), designated F_{ax}. [h] Unique axial environment of one F (type B), designated F_{ax}'. [i] Equatorial fluorine atom environments. [j] Phosphorus coupling with type A axial fluorine. [k] Phosphorus coupling with type B axial fluorine. [l] F_{ax}'-F_{eq} coupling constant. [m] F_{ax}-F_{eq} coupling constant. [n] Trans F_{ax}-F_{ax}' coupling constant. [o] Coupling between CF_3 group and the type A axial fluorines. [p] Coupling between the CF_3 group and the equatorial fluorine. [q] Coupling between the CF_3 group and the type B axial fluorine. [r] CH_3 on P. [s] CH_3 on S. [t] Axial CF_3 group. [u] Equatorial CF_3 group. [v] The axial CF_3 chemical shift is estimated because this portion of the spectrum is complex at this and lower temperatures. The coupling constants are reliable because they are clearly resolved in the ^{31}P spectrum.

Table II. Magnetization-Transfer Matrix for Concerted "BPR" and Rotation

	ee|a|a'	αα|α|α	αα|α|β	αα|β|α	αα|β|β	αβ|α|α	αβ|α|β	αβ|β|α	αβ|β|β	ββ|α|α	ββ|α|β	ββ|β|α	ββ|β|β
ee|a|a'													
αα|α|α	0	0	0	0	0	0	0	0	0	0	0	0	0
αα|α|β	0	-1.0	0	0	1.0	0	0	0	0	0	0	0	0
αα|β|α	0	0	-1.0	0	1.0	0	0	0	0	0	0	0	0
αα|β|β	0	0	0	-1.0	0	0	0	0	1.0	0	0	0	0
αβ|α|α	0	0.5	0.5	0	-1.0	0	0	0	0	0	0	0	0
αβ|α|β	0	0	0	0	0	-0.5	0.5	0	0	0	0	0	0
αβ|β|α	0	0	0	0	0	0.5	-0.5	0	0	0	0	0	0
αβ|β|β	0	0	0	0	0	0	0	-1.0	0	0.5	0.5	0	0
ββ|α|α	0	0	0	1.0	0	0	0	0	-1.0	0	0	0	0
ββ|α|β	0	0	0	0	0	0	0	1.0	0	-1.0	0	0	0
ββ|β|α	0	0	0	0	0	0	0	1.0	0	0	-1.0	0	0
ββ|β|β	0	0	0	0	0	0	0	0	0	0	0	0	0

broad doublet at low field ($\phi_F = 23.2$, $^1J_{PF} = 1000$ Hz), and (c) a single high-field broad band centered at 81.1 ppm which, considering the low temperature limiting ^{19}F spectrum, is best assigned as the high-field half of a second directly bound P–F resonance. At 273 K, therefore, axial and equatorial fluorine atoms are nonequivalent but fluorine exchange is occurring at intermediate rates and the lines are broad. The limiting low-temperature spectrum, obtained at 173 K, is consistent with the presence of four different fluorine environments arising from one equatorial fluorine (at high field), two different axial fluorines (at low field), and one equatorial CF_3 group also located toward the high-field region of the spectrum. Although accidental overlap of one portion of the equatorial F signal with the CF_3 signal occurs, both features can be clearly distinguished in the 173 K spectrum.

The proton-decoupled ^{31}P variable-temperature NMR spectra (Figure 6) were similarly interesting, consisting essentially of a quartet of quartets at 293 K. The intensity ratios and widths of the central quartets suggested that the deviations from ideality were due to a reduction of the rate of a molecular process, in particular the averaging of the three directly bound fluorine environments. The sharp quartet of quartets observed at 223 K is a consequence of the isolation of an equatorial fluorine environment with continued axial–axial fluorine exchange—that is "pseudorotation" has ceased but P–S bond rotation continues. The spectrum is best understood by inspection of the transfer matrices for the system (Table VI) because at 223 K the system is still in the intermediate exchange region. The matrix for "pseudorotation" (Table VIA) provides only two lines which are unaffected by exchange whereas the rotation process (with a static equatorial fluorine atom) provides a matrix (Table VIB) with four lines unperturbed by exchange. Each of these "lines" is of course a quartet group due to $^2J_{PF}$ coupling to the CF_3 group. Since the two groups of lines are defined by spin states differing only in the equatorial fluorine spin state, $^1J_{PF_{eq}}$ is visible at this temperature. The broad lines present in the 223 K spectrum are the lines affected by the rotation process, and this process can be analyzed independently from this point. At the lowest temperature, when all exchange has been stopped, these lines sharpen and the limiting spectrum shows each of the unique coupling constants. The limiting spectrum is composed of a double doublet of doublets, with each of these components further split into a quartet by the CF_3 coupling, giving a total of 32 lines (Figure 6).

There are therefore two discernible averaging processes in $CF_3PF_3(SCH_3)$, and the difference in the potential barriers between the two processes is sufficient to permit individual analysis. As in $F_4P(SCH_3)$, stopping only one of the processes cannot account for the splitting patterns and intensities observed in the ^{19}F and ^{31}P NMR spectra at the low-temperature limits. If the F ligand positional exchange in $CF_3PF_3(SCH_3)$

Table III. K Matrix for Axial-Equatorial F Exchange in F_4PSCH_3 (80% "Pseudorotation" and 20% Rotation)[a]

ee|a|a'	ee|a|α	αα|α|α	αα|α|β	αα|β|α	αα|β|β	αβ|α|α	αβ|α|β	αβ|β|α	αβ|β|β	ββ|α|α	ββ|α|β	ββ|β|α	ββ|β|β
αα|α|α	0	0	0	0	0	0	0	0	0	0	0	0	0
αα|α|β	0	-1.0	0.2	0	0.8	0	0	0	0	0	0	0	0
αα|β|α	0	0.2	-1.0	0	0.8	0	0	0	0	0	0	0	0
αα|β|β	0	0	0	-0.8	0	0	0	0	0.8	0	0	0	0
αβ|α|α	0	0.4	0.4	0	-0.8	0	0	0	0	0	0	0	0
αβ|α|β	0	0	0	0	0	-0.6	0.6	0	0	0	0	0	0
αβ|β|α	0	0	0	0	0	0.6	-0.6	0	0	0	0	0	0
αβ|β|β	0	0	0	0	0	0	0	-0.8	0	0.4	0.4	0	0
ββ|α|α	0	0	0	0.8	0	0	0	0	-0.8	0	0	0	0
ββ|α|β	0	0	0	0	0	0	0	0.8	0	-1.0	0.2	0	0
ββ|β|α	0	0	0	0	0	0	0	0.8	0	0.2	-1.0	0	0
ββ|β|β	0	0	0	0	0	0	0	0	0	0	0	0	0

[a] For the $^{31}P\{^1H\}$ spectrum.

Table IV. Activation Parameters of $F_4P(SCH_3)$ and (Trifluoromethyl)(methylthio)phosphoranes[a,b]

compd	E_a, kcal	$\Delta H^{\ddagger}$, kcal	$\Delta S^{\ddagger}$, eu	$\Delta G_T^{\ddagger}$ [c] (T_{av}), kcal	$\Delta G_{298}^{\ddagger}$, kcal	remarks
$F_4P(SCH_3)$	10.8 ± 0.2	10.4 ± 0.2	−2.0 ± 0.9	10.9 ± 0.3 (232)	11.0 ± 0.3	uncorrelated BPR and rotation
$(CF_3)_2PF_2(SCH_3)$	7.7 ± 0.1	7.3 ± 0.1	−9.2 ± 0.6	9.1 ± 0.2 (192)	10.0 ± 0.2	P-S bond rotation
$CH_3(CF_3)PF_2(SCH_3)$	10.1 ± 0.2	9.7 ± 0.2	−4.2 ± 0.7	10.6 ± 0.2 (215)	11.0 ± 0.3	P-S bond rotation
$CF_3PF_3(SCH_3)$	9.8 ± 0.2	9.3 ± 0.2	−2.9 ± 0.9	9.9 ± 0.2 (192)	10.2 ± 0.3	P-S bond rotation
	11.8 ± 0.4	11.3 ± 0.4	−5.0 ± 1.6	12.7 ± 0.6 (270)	12.8 ± 0.6	pseudorotation (BPR)
	12.1 ± 0.3	11.6 ± 0.3	−3.5 ± 1.0	12.5 ± 0.4 (238)	12.7 ± 0.4	*d*
$(CF_3)_3PF(SCH_3)$	13.6 ± 0.4	13.1 ± 0.4	5.4 ± 1.5	11.8 ± 0.5 (250)	11.5 ± 0.6	BPR of CF_3 groups

[a] Derived from ^{31}P line-shape analysis unless otherwise noted. [b] The limits of error given in this table are those derived from statistical analysis and do not include systematic errors. [c] Determined at the average temperature (T_{av}, K), which is not the coalescence temperature. [d] Obtained from the analysis of the CF_3 region of the ^{19}F spectrum which is sensitive only to the permutation (BPR) of the single fluorine nuclei.

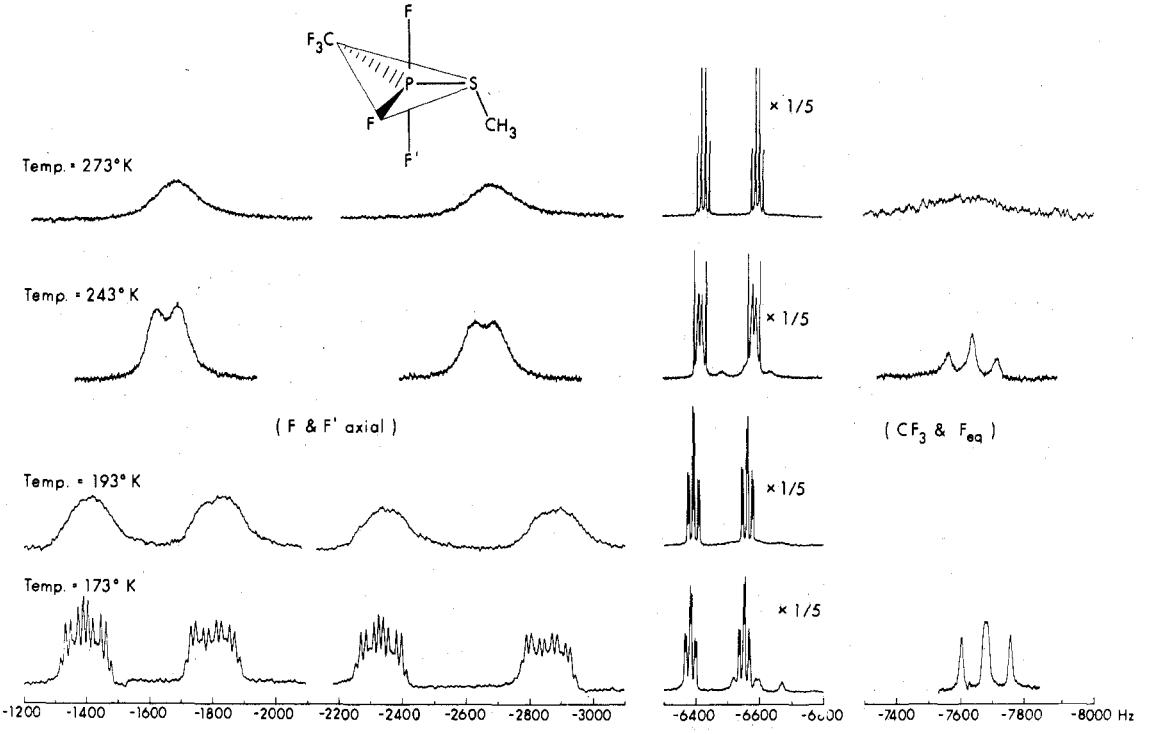

Figure 5. Temperature-dependent ^{19}F (94.1 MHz) CW NMR spectra of $CF_3PF_3(SCH_3)$. The intensity scale at each temperature is arbitrary but consistent as possible throughout each temperature. The strong CF_3 signals at −6500 Hz have been scaled down by a factor of 5. The scale gives offset frequencies relative to $CFCl_3$ reference.

Table V. K Matrix for Mutual Axial Fluorine Exchange in $CH_3(CF_3)PF_2(SCH_3)$[a] and $(CF_3)_2PF_2(SCH_3)$[b]

	a|a′			
a|a′	α|α	α|β	β|α	β|β
α|α	0	0	0	0
α|β	0	−1.0	1.0	0
β|α	0	1.0	−1.0	0
β|β	0	0	0	0

[a] One of four 4 × 4 submatrices for calculation of the $^{31}P\{^1H\}$ spectrum. The complete ^{31}P spectrum consists of a quartet due to coupling of the phosphorus with the CF_3 group. Complete reproduction of the $^{31}P\{^1H\}$ spectrum with all couplings requires that this matrix be repeated four times with line spacings given by $^2J_{PF}$. [b] One of seven 4 × 4 submatrices which is repeated seven times with spacing of $^2J_{PF}$ to reproduce the ^{31}P spectrum.

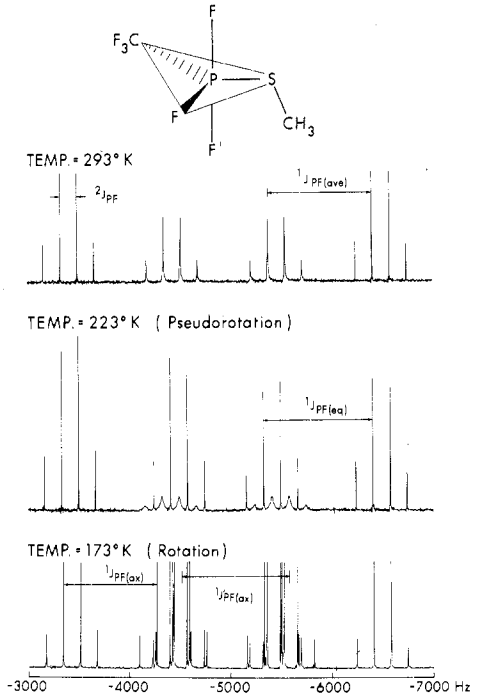

Figure 6. Proton-decoupled ^{31}P FT NMR spectra of $CF_3PF_3(SCH_3)$ at three temperatures. Coupling constants are shown in each segment. At 293 K, the coupling constants are averaged although exchange has not reached the fast limit. At 243 K, the lines unaffected by rotation are sharp while those affected by P–S rotation are broad. At 173 K, cessation of all processes (P–S rotation and pseudorotation) gives a spectrum described by the three limiting $^1J_{PF}$ coupling constants and the $^2J_{PF}$ coupling constant.

is considered only in terms of either the BPR or the TR mechanism,[10,11] then the latter would seem to be the more favorable route since it would preclude involvement of a "high-energy" species with CF_3 and SCH_3 in axial positions of the TBP. The present analysis cannot of course answer this question. Selected temperature-dependent ^{31}P NMR spectra used to determine the barriers are shown in Figure 7.

The averaging process also transforms the CF_3 signal from a doublet of quartets to a double doublet of triplets as the pseudorotation of directly bound fluorine atoms ceases. The differentiation of the axial F environments, due to P–S bond rotation, is not revealed in the CF_3 portion of the spectrum because the relevant couplings of the two axial fluorine environments are, within the resolution limits imposed by the breadth of the lines in this portion of the spectrum (~2 Hz), identical. Fitting this portion of the spectrum revealed a barrier in agreement with that obtained for "pseudorotation" from ^{31}P NMR.

D. Tris(trifluoromethyl)fluoro(methylthio)phosphorane, $(CF_3)_3PF(SCH_3)$. The proton-decoupled ^{31}P NMR spectrum of $(CF_3)_3PF(SCH_3)$ at 273 K consisted of a doublet of the

Table VI. K Matrices for Axial-Equatorial F Exchange in $CF_3PF_3(SCH_3)$[a]

A. Pseudorotation

	aa|e					
aa|e	αα|α	αα|β	αβ|α	αβ|β	ββ|α	ββ|β
αα|α	0	0	0	0	0	0
αα|β	0	−1.0	1.0	0	0	0
αβ|α	0	0.5	−0.5	0	0	0
αβ|β	0	0	0	−0.5	0.5	0
ββ|α	0	0	0	1.0	−1.0	0
ββ|β	0	0	0	0	0	0

B. P–SCH_3 Rotation with Distinct Axial Fluorines

	a|a′|e							
a|a′|e	α|α|α	α|α|β	α|β|α	α|β|β	β|α|α	β|α|β	β|β|α	β|β|β
α|α|α	0	0	0	0	0	0	0	0
α|α|β	0	0	0	0	0	0	0	0
α|β|α	0	0	−1.0	0	1.0	0	0	0
α|β|β	0	0	0	−1.0	0	1.0	0	0
β|α|α	0	0	1.0	0	−1.0	0	0	0
β|α|β	0	0	0	1.0	0	−1.0	0	0
β|β|α	0	0	0	0	0	0	0	0
β|β|β	0	0	0	0	0	0	0	0

[a] Each matrix is one of four submatrices. The quartet splitting of the spectrum arises from coupling of the phosphorus with the CF_3 group. Complete reproduction of the $^{31}P\{^1H\}$ spectrum requires that this matrix be repeated four times with line spacing determined by $^2J_{PF}$.

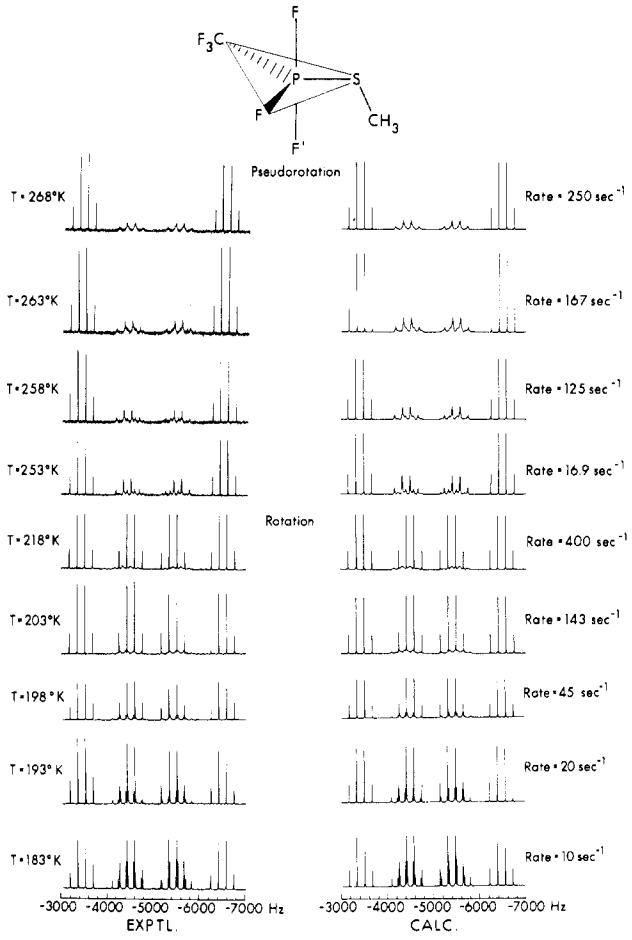

Figure 7. Experimental and calculated FT proton-decoupled ^{31}P spectra of $CF_3PF_3(SCH_3)$ through the two regions of visible processes (cessation of pseudorotation and rotation). Spectra were calculated by using the matrix of Table VI.

Table VII. Hydrolysis of (Trifluoromethyl)phosphoranes

	conditions	amt of compd, g (mmol)	yield, g (mmol) CF_3H	yield, g (mmol) CH_3SH	species in soln
$CF_3PF_3SCH_3$	neutral	0.169 (0.83)		*a*	F^-, BF_4^- *b,d*
	alkaline	0.107 (0.52)		*a*	$(CH_3S)_2$,*c* $CF_3PO_3^{2-}$ *d*
$CF_3(CH_3)PF_2SCH_3$	neutral	0.120 (0.60)		0.022 (0.46)	F^-,*e* HF_2^-,*f* $CH_3(CF_3)PO_2^-$
	alkaline (10%)	0.100 (0.50)	0.033 (0.47)	0.021 (0.44)	$CH_3(CF_3)PO_2^-$, F^-,*e* HF_2^- *f*
	satd NaOH		*a*	*a*	CH_3S^-, $CH_3PO_3^{2-}$, F^-, *e*
$(CF_3)_2PF_2(SCH_3)$	neutral	0.237 (0.93)	0.042 (0.59)		$CF_3PO_3^{2-}$, $CF_3PO_3H^-$
	alkaline	0.134 (0.53)	0.036 (0.51)	0.017 (0.35)	

a Observed but not quantitatively determined. *b* An unidentified species (ϕ_F = 74.8 ($CFCl_3$), J = 112 Hz) assigned to decomposition and not hydrolysis was also observed. *c* τ = 7.84. *d* Two minor P–F components, presumably decomposition products, were also observed. *e* ϕ_F = 120.9. *f* ϕ_F = 148.8.

central eight lines[19] of a decet, suggesting the equivalence of the three CF_3 groups. The breadth of the peaks suggested that the reduction of the rate of an exchange process is responsible for the appearance of the spectrum. The limiting spectrum, obtained at 213 K, indicated a ground-state structure with an axial F and one axial CF_3, with the assumption of a trigonal-bipyramidal framework.[2,4] The spectrum at 213 K comprised a doublet of the central five lines of a septet of quartets, arising from a splitting of P–F axial doublet components into a septet by the fluorines of the two equatorial CF_3 groups and further splitting into quartets by coupling of the axial CF_3 group. The magnetic equivalence of the three sets of CF_3 groups observed at higher temperatures is therefore likely due to a ligand rearrangement which averages the two CF_3 environments, a conclusion which is further supported by the fact that high-temperature $^2J_{PF}$ values are the weighted average of the limiting $^2J_{PF}$ coupling constants.[20]

It must be emphasized that the observed spectra have been investigated only between 263 and 213 K and do not provide any evidence for a fixed orientation of the SCH_3 group relative to the molecular plane. While we might have expected SCH_3 rotation to cease at very low temperatures, similar to the behavior of $(CF_3)_2PF_2(SCH_3)$ and $CH_3(CF_3)PF_3(SCH_3)$, it is not possible to extract this information in this case. The only process revealed by the NMR spectra of $(CF_3)_3PF(SCH_3)$ is the permutational interchange of CF_3 groups between axial and equatorial sites.

Computer simulation of the variable-temperature proton-decoupled ^{31}P NMR spectra at various rates gave spectra which could be fitted reasonably well to the experimental spectra, but the poor signal to noise ratio of the experimental spectra introduced a greater error in the fitting procedure and consequently in the $\Delta G_{298}^{\ddagger}$ value. The magnetization-transfer (**K**) matrix is given in the Appendix.[21]

E. Barrier Trends. Arrhenius plots are shown in Figure 8, and the barriers obtained are summarized in Table IV.

The $\Delta G_{298}^{\ddagger}$ value of 11.0 kcal obtained for $F_4P(SCH_3)$ is perhaps best ascribed to random, equally probable, rotation and "pseudorotation" processes which must both cease in order to yield the observed low-temperature limiting spectrum. The numerical value of the barrier is that given by the random processes although the correlated process yields similar values and also accounts for the gross features of the temperature-dependent spectrum. The barrier to "pseudorotation" in $F_4P(SCH_3)$ is larger than that for $F_4PN(CH_3)_2$, in contrast to the earlier suggestion,[18] without barrier analysis support, that the reverse order prevailed. Clearly more numerical results are necessary to illuminate the barrier trends in the XPF_4 system; the qualitative estimations employed to date for many of the systems are clearly inadequate.

Rotational barriers of 11.0 kcal for $CH_3(CF_3)PF_2(SCH_3)$ and 10.0 kcal for $(CF_3)_2PF_2(SCH_3)$ are close to the barrier obtained for $F_4P(SCH_3)$ which includes a P–S bond rotation component.

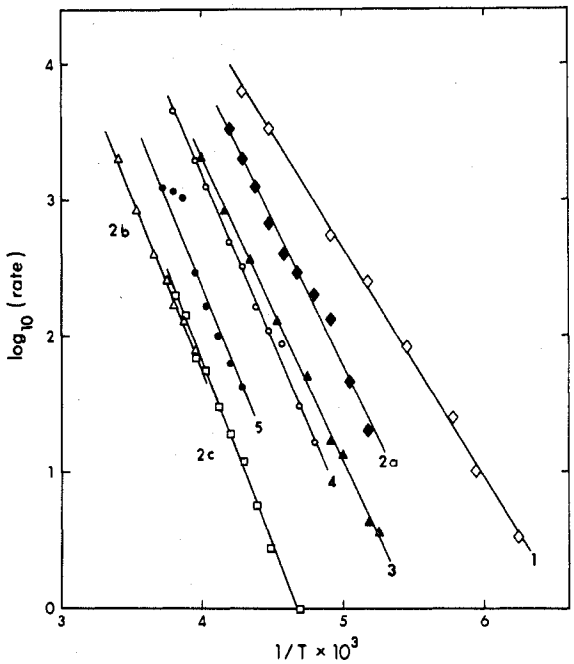

Figure 8. Arrhenius plots for the ^{31}P dynamic NMR analysis of the compounds studied herein: (1) $(CF_3)_2PF_2(SCH_3)$; (2) $CF_3PF_3(SCH_3)$ for (a) rotation and (b) pseudorotation [the line labeled 2c represents the fit of the CF_3 (^{19}F) spectrum of $CF_3PF_3(SCH_3)$ which is sensitive only to the cessation of pseudorotation in the molecule]; (3) $CH_3(CF_3)PF_2(SCH_3)$; (4) $F_4P(SCH_3)$; (5) $(CF_3)_3PF(SCH_3)$.

Of the two barriers obtained for $CF_3PF_3(SCH_3)$ the value of 10.2 kcal ascribed to the rotation process is in good agreement with the values derived above. The higher barrier, 12.8 kcal, is best assigned to the process (BPR etc.) which is thought to be responsible for scrambling the directly bound fluorine atoms. The barrier to pseudorotatory processes appears to be generally higher for PF_3X_2 systems than for the corresponding XPF_4 compounds.[2,14,21] It is notable that the "pseudorotation" barrier in $CF_3PF_3(SCH_3)$ (12.8 kcal) is smaller than that for $CF_3PF_3N(CH_3)_2$ (15.6 kcal),[22] in opposition to the order of the barriers in the XPF_4 analogues discussed above.

The barrier of 11.5 kcal for the averaging process in $(CF_3)_3PF(SCH_3)$, which is assigned to pseudorotatory interchange of CF_3 groups between axial and equatorial environments, is smaller than that obtained recently[2] for the similar process in $(CF_3)_3CH_3P(SCH_3)$, 15.5 kcal. The difference in values is significant in spite of the larger error in the former. Replacement of a CH_3 group by a halogen appears to reduce the barrier,[2] as demonstrated by these two compounds. Notably similar barriers to pseudorotation are exhibited by these and related compounds,[2,14,22] indicating that the energy barriers are not greatly dependent on the mass of the substituent.

There are few previous data available for P–S bond rotation

barriers in P^V (or P^{III}) systems.[23] The present values appear to be reasonable and indicate that both systems possess similar barriers.[2,22,24-26] While it has been suggested that these barriers arise from π bonding,[25] the question remains unsettled.[18]

Experimental Section

Instrumentation. All manipulations were carried out in a Pyrex vacuum system equipped with vacuum taps greased with Apiezon N stopcock grease. Separations were effected by means of cold "slush" baths prepared from frozen organic solvents.

Infrared spectra were taken with a Perkin-Elmer 421 infrared spectrometer using a 9-cm gas cell equipped with KBr windows. NMR spectra were obtained with a Varian HA 100 or Bruker HFX 90 spectrometer, the former (^1H, 100.1 MHz; ^{19}F, 94.1 MHz) operating in CW mode with homonuclear lock and the latter (^{31}P, 36.4 MHz) in the pulsed FT mode with heteronuclear lock. Samples were prepared under vacuum in sealed tubes as approximately 10% solutions in CCl_3F with, in the case of ^{31}P spectra, added proportions of CD_2Cl_2 for ^2D lock. Chemical shifts are referred to $(CH_3)_4Si$ (^1H), CCl_3F (^{19}F), or P_4O_6 (^{31}P)[27] standards, positive values denoting resonances to high field of the standard. Temperature-dependent spectra were obtained on both instruments equipped with the Bruker temperature controller, the accuracy of which was established by separate calibration. Separate experiment showed that no detectable temperature gradients existed in the sample tubes. Measurement of some exchange rates at different concentrations indicated that, within the accessible concentration range, the process is concentration independent. No significant variation in line width or chemical shift with temperature was observed.

Mass spectra were obtained with an AEI MS9 instrument at an ionizing voltage of 70 eV, using a specially designed direct-inlet system to introduce the compound.

Preparations. (a) $F_4P(SCH_3)$. $F_4P(SCH_3)$ was prepared by cocondensing a 1:1 mole ratio of $(CH_3)_3Si(SCH_3)$ and PF_5 in a 10-mL reaction tube, which was then sealed under vacuum and maintained in an ice–water bath for 30 min. The volatile products were then separated by passing the volatile materials through a series of traps maintained at −63, −78, −96, and −196 °C.[3] The bulk of $F_4P(SCH_3)$ was trapped at −78 °C. A second separation treatment of the material trapped at −78 °C removed the remaining traces of $(CH_3)_3SiF$, the other major product of the reaction. All NMR spectra of $F_4P(SCH_3)$ were obtained below 273 K because of the known[3] instability of this compound.

(b) $CF_3PF_3(SCH_3)$. $CF_3PF_3(SCH_3)$ was synthesized in a manner similar to that described above, using a 1:1 mole ratio of CF_3PF_4 and $(CH_3)_3Si(SCH_3)$. The reaction system was maintained at −23 °C for 1 h. Vacuum separation of volatile products yielded $CF_3PF_3(SCH_3)$, which was collected at −78 °C, $(CH_3)_3SiF$, which was collected at −96 °C, and unreacted CF_3PF_4, which was collected at −196 °C. The product was characterized by its hydrolysis reactions in both neutral and basic mediums (Table VII).

(c) $CF_3(CH_3)PF_2(SCH_3)$. $CH_3(CF_3)PF_3$ (0.275 g, 1.60 mmol) was treated with $(CH_3)_3Si(SCH_3)$ (0.147 g, 1.23 mmol) at room temperature. After agitation of the mixture for 2 days, the products were separated as above. The bulk of the desired product, $CH_3(CF_3)PF_2(SCH_3)$, was collected in the −45 °C trap. A small amount passed through into the −63 °C trap, giving, in total, a quantitative yield (0.248 g, 1.24 mmol, 100%) of $CF_3(CH_3)PF_2(SCH_3)$. The remaining volatile fractions consisted of $(CH_3)_3SiF$ and excess $CH_3(CF_3)PF_3$ (total mass 0.179 g).

NMR spectral data for $CH_3(CF_3)PF_2(SCH_3)$ are given in Table I and hydrolysis results in Table VII. The infrared spectrum showed the following prominent bands (with principal assignments): 2976 (m), 2951 (m), 2771 (w) (ν(CH)); 1436 (m), 1316 (w) ($\sigma_{asym}(CH_3)$); 1266 (s); 1214 (s), 1196 (s), 1147 (s), 1076 (vw), 1027 (vs) (ν(CF)); 971 (m), 891 (s), 859 (s) (ν(PF)); 799 (s), 769 (s) ($\sigma_{asym}(CF_3)$); 712 (m), 693 (m), 607 (m), 583 (s), 471 (s) cm^{-1}.

The SCD_3 analogue was prepared in the same fashion: $CH_3(CF_3)PF_3$ (0.140 g, 0.813 mmol) was condensed upon $(CH_3)_3Si(SCD_3)$ (0.087 g, 0.706 mmol) [prepared by reacting $(CH_3)_3SiN(CH_3)_2$ (1.330 g, 11.4 mmol) with CD_3SH (0.647 g, 12.7 mmol) for 3 days at room temperature, the yield of the deuterated silyl thioether being 75.6% on the basis of the initial amount of $(CH_3)_3SiN(CH_3)_2$ used], and the reaction vessel was agitated for 2 h at 0 °C. A 98% yield (0.139 g, 0.685 mmol) of the deuteriothiomethylated phosphorane, based on $(CH_3)_3Si(SCD_3)$ consumed, was obtained. Comparison of the ^1H NMR spectra of both derivatives allowed the unambiguous assignment of the NMR signal due to CH_3 attached to phosphorus.

(d) $(CF_3)_2PF_2(SCH_3)$. $(CF_3)_2PF_3$ (0.709 g, 3.14 mmol) and $(CH_3)_3Si(SCH_3)$ (0.276 g, 2.30 mmol) were sealed in a tube and allowed to react at room temperature for 1 h. Separation of volatile products under vacuum gave $(CF_3)_2PF_2(SCH_3)$ (0.565 g, 2.22 mmol, 80% yield), unreacted $(CF_3)_2PF_3$, and $(CH_3)_3SiF$. Hydrolysis results are given in Table VII.

(e) $(CF_3)_3PF(SCH_3)$.[4] $(CF_3)_3PF_2$ (1.26 g, 4.56 mmol) and $(CH_3)_3Si(SCH_3)$ (0.501 g, 4.19 mmol) were combined in a sealed tube and allowed to react slowly while being warmed from −78 to −15 °C over a 1-day period. Separation of the volatile products under vacuum gave $(CF_3)_3PF(SCH_3)$ (1.16 g, 3.5 mmol, 82% yield) plus $(CH_3)_3SiF$.

Acknowledgment. We thank the National Research Council of Canada for financial support of this work.

Registry No. $F_4P(SCH_3)$, 22606-68-4; $CF_3PF_3(SCH_3)$, 71411-44-4; $CF_3(CH_3)PF_2(SCH_3)$, 71411-45-5; $(CF_3)_2PF_2(SCH_3)$, 71411-46-6; $(CF_3)_3PF(SCH_3)$, 51874-42-1; PF_5, 7647-19-0; CF_3PF_4, 1184-81-2; $CH_3(CF_3)PF_3$, 69517-31-3; $(CF_3)_2PF_3$, 1184-82-3; $(CF_3)_3PF_2$, 661-45-0; $(CH_3)_3Si(SCH_3)$, 3908-55-2.

Supplementary Material Available: The reduced (40 × 40) magnetization-transfer (**K**) matrix (1 page). Ordering information is given on any current masthead page.

References and Notes

(1) Presented in part at the 172nd National Meeting of the American Chemical Society, San Francisco, CA, Aug 30–Sept 3, 1976.
(2) R. G. Cavell, J. A. Gibson, and Kwat I. The, *Inorg. Chem.*, **17**, 2880 (1978).
(3) S. C. Peake and R. Schmutzler, *J. Chem. Soc. A*, 1049 (1970).
(4) Kwat I. The and R. G. Cavell, *Inorg. Chem.*, **15**, 2518 (1976).
(5) R. B. Johannesen, S. C. Peake, and R. Schmutzler, *Z. Naturforsch., B*, **29**, 699 (1974).
(6) Access to the program NUMARIT by John S. Martin, University of Alberta, and K. Worvall, University of East Anglia, was kindly provided by J.S.M.
(7) The spectra reported in ref 5 were obtained without the use of a signal lock.
(8) Inversion at divalent sulfur and P–S bond rotation are permutationally equivalent processes for the five-coordinate phosphorus molecules and thus cannot be distinguished by the NMR experiment. Although little is known about inversion of dicoordinate sulfur, we suspect that the barrier to this process is higher[9] than that of rotation about the P–S bond; hence we visualize the latter as the effective process.
(9) See for example H. Kessler, *Angew. Chem.*, **82**, 237 (1970); *Angew. Chem., Int. Ed. Engl.*, **9**, 219 (1970).
(10) R. S. Berry, *J. Chem. Phys.*, **32**, 933 (1960).
(11) I. Ugi, D. Marquarding, H. Klusacek, P. Gillespie, and F. Ramierz, *Acc. Chem. Res.*, **4**, 288 (1971).
(12) A locally adapted version of the program EXCHSYS described by J. K. Kreiger, J. M. Deutsch, and G. M. Whitesides, *Inorg. Chem.*, **12**, 1535 (1973), was used for the calculations. Details of the program and the description of the construction of the kinetic magnetization-transfer matrix are given in the thesis of J. K. Kreiger, M.I.T., Cambridge, MA, 1971.
(13) W. Klemperer in "Dynamic Nuclear Magnetic Resonance Spectroscopy", L. M. Jackman and F. A. Cotton, Eds., Academic Press, New York, 1975, Chapter 2.
(14) C. G. Moreland, G. O. Doak, L. B. Littlefield, N. S. Walker, J. W. Gilge, R. W. Braun, and A. H. Cowley, *J. Am. Chem. Soc.*, **98**, 2161 (1976).
(15) J. I. Musher, *J. Am. Chem. Soc.*, **94**, 5662 (1972).
(16) K. Laidler, "Chemical Kinetics", McGraw-Hill, New York, 1950.
(17) A. Allerhand, H. S. Gutowsky, J. Jonas, and R. A. Meinzger, *J. Am. Chem. Soc.*, **88**, 3195 (1966); G. Binsch in "Dynamic Nuclear Magnetic Resonance Spectroscopy", L. M. Jackman and F. A. Cotton, Eds., Academic Press, New York, 1975, Chapter 3.
(18) M. Eisenhut, H. L. Mitchell, D. D. Traficante, R. J. Kaufman, J. M. Deutsch, and G. M. Whitesides, *J. Am. Chem. Soc.*, **96**, 5385 (1974).
(19) The experimental intensity ratio is in agreement with that for the central eight lines of a decet rather than a true octet.
(20) R. G. Cavell, J. A. Gibson, and Kwat I. The, *J. Am. Chem. Soc.*, **99**, 7841 (1977).
(21) Supplementary material.
(22) R. G. Cavell, N. T. Yap, L. Vande Griend, K. I. The, and J. A. Gibson, unpublished work.
(23) A barrier of 5.2 kcal for P–S bond rotation in $C_6H_5PF_3SC_2H_5$ was given by M. A. Sokal'skii, G. I. Drozd, M. A. Landau, and S. S. Dubov, *Zh. Strukt. Khim.*, **10**, 1113 (1969) [*J. Struct. Chem. (Engl. Trans.)*, **10**, 993 (1969)]. This value appears to be low in comparison with the present work.
(24) Some examples of P–N rotation barriers are given by the following: A. H. Cowley, M. J. S. Dewar, W. R. Jackson, and W. B. Jennings, *J. Am. Chem. Soc.*, **92**, 1085, 5206 (1970); R. H. Nielson, R. Chung-Yi Lee,

and A. H. Cowley, *ibid.*, **97**, 5302 (1975); S. Distefano, H. Goldwhite, and E. Mazzola, *Org. Magn. Reson.*, **6**, 1 (1974).
(25) E. L. Muetterties, P. Meakin, and R. Hoffmann, *J. Am. Chem. Soc.*, **94**, 5674 (1972).
(26) R. Hoffmann, J. M. Howell, and E. L. Muetterties, *J. Am. Chem. Soc.*, **94**, 3047 (1972); A. Rauk, L. C. Allen, and K. Mislow, *ibid.*, **94**, 3035 (1972); A. Stritch and A. Veillard, *ibid.*, **95**, 5574 (1973).
(27) A. C. Chapman, J. Horner, D. J. Mowthorpe, and K. T. Jones, *Chem. Commun.*, 121 (1969). The chemical shift of 85% H_3PO_4 is +112 ppm vs. P_4O_6.

Contribution No. 2592 from the Central Research and Development Department, Experimental Station, E. I. du Pont de Nemours and Company, Wilmington, Delaware 19898

Application of Molecular Orbital Theory to Transition-Metal Complexes. 1. Fully Optimized Geometries of First-Row Metal Carbonyl Compounds

DAVID A. PENSAK* and RONALD J. McKINNEY

Received December 21, 1978

Extended Hückel theory, modified with the inclusion of two-body repulsion, has been used to reproduce and predict optimum geometries, *including bond lengths*, of some first-row transition metal carbonyl compounds.

Introduction

The application of molecular orbital (MO) techniques to transition-metal complexes is an increasingly active field.[1] In general, studies have focused on bonding in organometallic complexes and how such bonding is influenced by changes in the coordination sphere. A few papers have contained an examination of bonding changes during chemical reactions.[2]

We are interested in using MO calculations as a practical guide for laboratory studies. It is our goal to develop the capability for theoretical studies of, for example, relative rates of reaction or the comparison of first- and second-order substitution pathways. Ultimately this might facilitate the design of reagents for specific chemical transformations. Though it is widely held that only the more sophisticated nonempirical MO techniques can give reasonable results, recent work has demonstrated that semiempirical techniques can make significant contributions in this area.[3] This is important in terms of cost, computer time, and simplicity if such calculations are to become a routine tool of the experimentalist.

Throughout this work a semiempirical MO theory as derived by Anderson is used.[4] It is similar to extended Hückel theory (EHT)[5] but contains a correction for two-body repulsion. While the modified extended Hückel theory (MEHT) retains the ability of EHT to reproduce bond angles, it markedly improves bond length determinations. MEHT has been applied to the interaction of small molecules with metal clusters and surfaces as well as with a few organometallic derivatives.[6]

In this and future papers, we will use the MEHT approach to determine the relative energies of complexes in ground, intermediate, and transition states[7] and will be less concerned with a detailed MO analysis of the causes of geometry and bonding. We will demonstrate that for certain classes of complexes, reliable results can be obtained. In the present paper we will examine the ability of MEHT to predict correct bond distances and angles of some simple metal carbonyl derivatives and fragments and compare the results with previous EHT studies by Elian and Hoffmann[8] and by Burdett.[9] In the companion paper,[10] we will compare calculated energies against known thermodynamic values for some dissociative processes.

Results

A. $M(CO)_6$. Octahedral symmetry requires that only bond lengths be optimized. The optimized metal–carbon distances for one d^5 [M = V(0)] and three d^6 [M = V(−I), Cr(0), Mn(I)] metal complexes are 1.87, 1.86, 1.86, and 1.87 Å, respectively, with corresponding optimized carbon–oxygen distances of 1.10, 1.11, 1.12, and 1.12 Å. For vandium(0) and chromium(0), both the metal–carbon and carbon–oxygen distances are shorter than those of the experimental values [V–C = 2.015 (2) Å, C–O = 1.138 (2) Å;[11] Cr–C = 1.91 (4) Å, C–O = 1.14 (4) Å[12]]. This is somewhat exceptional—more often the optimized bond lengths are longer than experimentally observed distances (vide infra).

In the d^5 vanadium(0) case, the octahedral geometry should be unstable due to first-order Jahn–Teller effects. In accordance with the distortion expected on the basis of ligand field theory, i.e., a shortening of a trans pair of metal–carbon bonds relative to the other bonds,[13] the geometry of vanadium hexacarbonyl was also optimized under D_{4h} symmetry. The axial vanadium–carbon distances shortened from 1.87 to 1.85 Å while the equatorial vanadium–carbon distances lengthened to 1.88 Å. However, the D_{4h} geometry was calculated to be only about 0.5 kcal/mol more stable than the O_h geometry. While we have not attempted to calculate a complete Jahn–Teller surface, the small energy difference between O_h and D_{4h} geometries is not inconsistent with the observation that the predicted Jahn–Teller effect is small enough to give rise, experimentally, to a dynamic effect.[9] The ability to explore Jahn–Teller distortions is a potential strength of geometry-optimized MEHT calculations.

B. $M(CO)_5$. Geometries in $M(CO)_5$ complexes were optimized under both D_{3h} (trigonal bipyramidal), **1**, and C_{4v} (square pyramidal), **2**, symmetry restrictions. In several

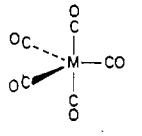

1, D_{3h}

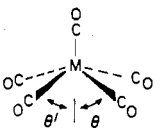

2, C_{4v} $\theta = \theta'$
3, C_{2v} $\theta \neq \theta'$

studies using semiempirical[8,9] and ab initio[14,15] techniques, the molecular orbitals generated under these two symmetries have been detailed. In general, our results are in agreement with previous findings and, with a few exceptions, the known structural data.[16-20] The optimized bond distances and angles are presented in Table I. Demuynck, Strich, and Veillard,[14] using large basis set ab initio techniques, have also optimized metal–carbon bond lengths and angles for several of the same complexes and their results are included in Table I in brackets.

0020-1669/79/1318-3407$01.00/0